Larhyss Journal, ISSN 1112-3680, n°63, Sep 2025, pp. 135-154

DIMENSIONLESS MODELING OF SUBMERGED FLOW CONDITIONS IN SMALL OVERFLOW DAMS

ACHOUR B.[1*], HOUICHI L.[2]

[1] Professor, Research Laboratory in Subterranean and Surface Hydraulics (LARHYSS), University of Biskra, PO Box 145 RP, Biskra, Algeria
[2] Professor, Hydraulic Department, Faculty of Technology, University of Batna 2, Algeria

(*) bachir.achour@larhyss.net

Research Article – Available at http://larhyss.net/ojs/index.php/larhyss/index
Received October 21, 2024, Received in revised form August 22, 2025, Accepted August 24, 2025

ABSTRACT

This paper presents a novel theoretical investigation into the hydraulic behavior of small overflow dams operating under *submerged* flow conditions. Motivated by the lack of analytical tools tailored to this class of hydraulic structures, the study introduces a dimensionless modeling framework capable of predicting the transition between *submerged* and free-flow regimes. The methodology is rooted in fundamental hydraulic principles, particularly the conservation of energy and continuity, under the assumption that frictional losses are negligible - a valid simplification for small-scale dams.

Key dimensionless parameters are defined, notably the upstream depth ratio $z = h/s$, the unit discharge intensity parameter $\psi = q / (\sqrt{2g}\, s^{3/2})$, and the downstream depth ratio $w = h_1/(s + h)$, where h is the upstream flow depth above the dam crest, s is the dam's height, q is the unit discharge, h_1 is the downstream flow depth at the toe of the small dam, and g is the acceleration due to gravity. Using these, the authors derive second-order equations that yield explicit expressions for determining the flow regime, the downstream flow depth, and the submergence ratio β. A critical outcome is the identification of a unique predictive curve that separates *submerged* from *unsubmerged* conditions in the (ψ, z) domain. This theoretical boundary enables practitioners to rapidly diagnose the hydraulic status of a small dam using basic input parameters.

The study further demonstrates that the downstream depth ratio w is governed by a second-order equation, the solution of which yields an explicit expression for computing w based on known values of ψ and z.

A relevant relationship is proposed enabling computing the downstream flow depth at the toe of the small depth, using only a minimal set of known dimensionless key parameters, namely, ψ, s, and z.

Further, the paper introduces and analytically formulates the submergence ratio β, which encapsulates the influence of downstream conditions on the overall flow behavior. This parameter, provides engineers with a robust and intuitive framework for the operational assessment of small overflow dams, especially the nature of the flow.

The proposed methodology avoiding empirical calibration, is generalizable across a wide range of dam configurations, and enhances decision-making in both design and field applications. In doing so, this work fills a significant gap in the hydraulic literature and offers a practical yet theoretically rigorous solution to the challenge of assessing *submerged* flow conditions in small hydraulic structures.

It is noteworthy that the present study, grounded in the authors' own earlier foundational work, advances a renewed perspective - placing particular emphasis on delivering more nuanced qualitative interpretations of the hydraulic phenomena and the parameters that govern them.

Keywords: Overspill dam, Small dam, Submergence rate, Downstream depth ratio, Sill, Unit flow discharge.

INTRODUCTION

The study of flow over hydraulic structures is fundamental to the design and operation of dams, weirs, and related water conveyance systems. Among these structures, small overflow dams serve essential roles in irrigation, flood control, and water measurement. A critical aspect in their hydraulic behavior is the distinction between *submerged* and *unsubmerged* flow regimes, as the operational state of a dam directly influences discharge capacity, backwater effects, and downstream energy dissipation mechanisms. Despite their practical importance, the flow characteristics over small *submerged* overflow dams remain underexplored in the literature.

In the case of an *unsubmerged* weir, the flow rate depends both on the weir's geometry and on the upstream flow conditions. The head-discharge relationship is influenced by the shape of the weir crest, the total energy head above the crest, as well as the height and width of the weir (Falvey, 2003; Bazin, 1894; Cox, 1928; Rehbock, 1929; Achour et al., 2003; Bos, 1976; SIA, 1936). When the approach flow velocity becomes negligible, the total head is typically replaced by the flow depth, always measured relative to the crest elevation.

As for *submerged* flow, several studies have focused on establishing discharge relationships for thin-crested linear weirs (Fteley and Stearns, 1883; Francis, 1884; Bazin, 1894; Cox, 1928; Villemonte, 1947). In fact, it is the ratio Q/Q_0, known as the flow reduction factor, that is determined as a function of the submergence factor h_2/h_1. The discharge Q corresponds to the flow over the *submerged* weir, while Q_0 refers to the discharge over an *unsubmerged* weir associated with the upstream depth h_1. Here, h_2 represents the downstream flow depth of the *submerged* flow measured from the weir crest, and h_1 denotes the upstream flow depth above the crest of the *submerged* weir. Bazin's results (1894) did not lead to a single and unified expression for the flow reduction factor; rather, they produced a family of curves based on the ratio P/h_1, where P is the height of the weir, denoted s in the present study.

Historically, *submerged* flow conditions have been well documented for sharp-crested weirs used in open channel discharge measurement (Villemonte, 1947). Submergence occurs when the downstream water surface rises above the weir crest, thereby impeding the free fall of water and reducing the effective discharge. Conversely, *unsubmerged* or free-flow conditions allow full discharge potential, uninfluenced by downstream levels. While several classical studies (Fteley and Stearns, 1883; Francis, 1884; Bazin, 1894; Cox, 1928; Villemonte, 1947) have contributed to the characterization of these regimes in the context of thin-crested weirs, their findings often lack direct applicability to small dam structures due to geometric and hydraulic differences.

In particular, Bazin's pioneering work (1894) highlighted the variability of discharge under *submerged* conditions, offering a series of curves rather than a universal formula. His results introduced the concept of a *reduction factor*, a function of submergence depth and weir height. However, they did not establish a precise criterion for defining the transition between flow regimes nor did they address the specific context of small spillway dams. Bazin's results (1894) did not lead to a single and unified expression for the flow reduction factor; rather, they produced a family of curves based on the ratio P/h_1.

Similarly, modern references such as Falvey (2003) focus on the design of labyrinth weirs or complex structures, providing limited guidance for straightforward submergence assessments in small dams.

Recognizing this gap, the present study proposes a dimensionless theoretical framework tailored to small overflow dams operating under *submerged* or transitional flow regimes. Unlike empirical or experimental approaches, this research is grounded in analytical hydrodynamics. Assuming negligible the effects of frictional losses along the downstream slope, a valid approximation for small dams - the study derives a set of governing equations from energy principles and continuity considerations.

Fundamental hydraulic principles are employed to delineate the limit between *submerged* and *unsubmerged* flow regimes. An explicit relationship, expressed through a single representative curve, is developed to predict whether the overflow dam operates under *submerged* or free-flow conditions. Building on clearly defined parameters, the study further proposes explicit theoretical equations for determining both the downstream depth ratio and the submergence ratio of the overflow dam.

Key contributions of the paper include the development of a second-order equation that explicitly defines the submergence threshold, enabling a precise classification of flow conditions. Moreover, by introducing three core dimensionless parameters - ψ (representing flow intensity), z (upstream flow depth ratio), and w (downstream flow depth ratio) - the study constructs a generalizable model applicable to a variety of practical scenarios. These parameters are used to produce concise and practical graphical tools, allowing for rapid diagnosis of submergence without resorting to iterative or site-specific calibration procedures.

Finally, the work defines a new dimensionless indicator, the *submergence ratio β*, which offers engineers an intuitive and quantitative metric for evaluating the degree of downstream influence on discharge. Through theoretical derivation and graphical analysis, the paper delivers not only a robust conceptual framework but also pragmatic tools to support hydraulic design, performance evaluation, and operational management of small overflow dams.

It is worth noting that the present study, building upon the foundational research conducted by Achour and Houichi (2019), offers a renewed perspective, with particular emphasis on providing more refined qualitative interpretations of the hydraulic phenomena involved and their governing parameters.

LIMIT OF SUBMERGED SMALL DAM FLOW

Fig. 1 illustrates a small dam of height s overtopped by a flow depth h. Upstream of the dam, the approach flow velocity head is denoted by $V^2/2g$. The flow downstream of the dam toe has a depth h_1 and a main velocity V_1. The discharge passing over the weir is denoted Q.

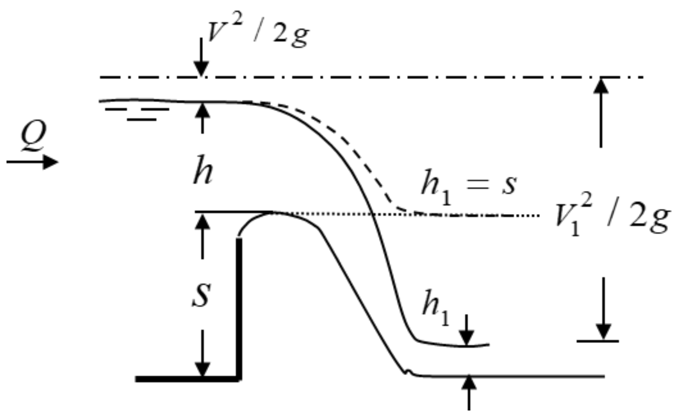

Figure 1: Definition sketch of flow over the small dam under consideration

Between the upstream and downstream sections of the dam, the following total energy head equality can be written as follows (Fig. 1):

$$s + h + \frac{V^2}{2g} = h_1 + \frac{V_1^2}{2g} \tag{1}$$

Note that the effects of friction losses along the downstream face are neglected due the small dimensions of the dam.

Introducing into Eq. (1) the following well established equations $V = Q / A$ and $V_1 = Q / A_1$, where A and A_1 are the water areas upstream and downstream of the dam, respectively, one may write the following:

$$s + h + \frac{Q^2}{2gA^2} = h_1 + \frac{Q^2}{2gA_1^2} \tag{2}$$

The water area A and A_1 can be respectively expressed as $A = (s + h)B$ and $A_1 = Bh_1$ where B is the dam width. Thus, Eq. (2) can be rewritten as follows:

$$s + h + \frac{Q^2}{2g(s+h)^2 B^2} = h_1 + \frac{Q^2}{2gB^2 h_1^2} \tag{3}$$

The limit condition for the *submerged* dam corresponds to the following equality (Fig.1):

$$h_1 = s \tag{4}$$

Introducing into Eq. (3) the discharge $q = Q/B$ per unit width of the dam, and Eq. (4), yields the following:

$$s + h + \frac{q^2}{2g(s+h)^2} = s + \frac{q^2}{2gs^2} \tag{5}$$

After simplifications, Eq. (5) becomes as follows:

$$h + \frac{q^2}{2g(s+h)^2} = \frac{q^2}{2gs^2} \tag{6}$$

On the other hand, Eq. (6) can be written in the following form:

$$h + \frac{q^2}{2gs^2\left(1 + \frac{h}{s}\right)^2} = \frac{q^2}{2gs^2} \tag{7}$$

Dividing both sides of Eq. (7) by s, the following is obtained:

$$\frac{h}{s}+\frac{q^2}{2gs^3\left(1+\frac{h}{s}\right)^2}=\frac{q^2}{2gs^3} \tag{8}$$

Note that the unit discharge q simplifies the analysis of flow over structures like weirs and spillways by normalizing the discharge with respect to the width, allowing the problem to be treated as a two-dimensional flow in many cases.

For the sake of notational simplicity, let us define the following dimensionless parameters:

$\psi=\frac{q}{\sqrt{2g}s^{3/2}}$, and $z=\frac{h}{s}$

The dimensionless parameter ψ can be meaningfully referred to as "the unit discharge intensity parameter" for the following physical reasons. It reflects the normalization by gravitational and geometric scales. The denominator $\sqrt{2g}s^{3/2}$ introduces a characteristic flow scale that reflects the potential energy associated with the dam height s. By dividing the unit discharge q by this term, ψ effectively measures how intense the incoming flow is relative to the hydraulic capacity of the structure. While not a standard term, "flow intensity" can be interpreted as a measure of the flow rate per unit width, which is exactly what the unit discharge q represents. Therefore, in this context, the unit discharge q can be considered as a measure of flow intensity.

The previous definition of the dimensionless ψ is a dimensionless expression of flow strength. Indeed, the expression of ψ carries no units, allowing it to act as a pure indicator of hydraulic regime. It combines physical inputs, discharge, gravity, and crest geometry, into a single parameter that captures the hydrodynamic force of the incoming flow in relation to structural constraints. It represents also an indicator of flow regime and submergence potential. In the context of *submerged* or *unsubmerged* flow over small dams, ψ is a critical input in defining the downstream response. A higher ψ implies a more forceful incoming flow that is more likely to cause submergence, especially for smaller dam heights. Therefore, it is key to determining the onset and degree of submergence.

Even as the square root of a kinetic-to-potential energy ratio, ψ maintains a clear physical meaning: it quantifies the relative intensity of the unit discharge normalized by a structural and gravitational baseline. This makes it not only a valid but also a very insightful dimensionless parameter for modeling and classifying flow conditions over small overflow dams.

Given its role in comparing flow energy per unit width to the structural scale of the dam, and its ability to indicate hydraulic behavior under varying discharge conditions, calling

ψ the "unit discharge intensity parameter" is both physically justified and conceptually appropriate.

Introducing the previous relationships defining the parameters ψ and z into Eq. (8), yields what follows:

$$z+\frac{\psi^2}{(1+z)^2}=\psi^2 \tag{9}$$

After rearrangement, the following second-degree equation in z is obtained:

$$z^2+\left(2-\psi^2\right)z+\left(1-2\psi^2\right)=0 \tag{9a}$$

The discriminant of Eq. (9) is given by the following relationship:

$$\Delta=\left(2-\psi^2\right)^2-4\left(1-2\psi^2\right)$$

The calculation shows that, regardless of the value of ψ, the discriminant is positive. The real root of Eq. (9) is therefore given by what follows:

$$z=\frac{h}{s}=\frac{\psi^2}{2}+\sqrt{\left(1-\psi^2/2\right)^2+2\psi^2-1}\quad-1 \tag{10}$$

Eq. (10) is valid for $\psi \geq \sqrt{2}/2$.

The small dam is then considered *submerged* when the following inequality is satisfied:

$$z=\frac{h}{s}<\frac{\psi^2}{2}+\sqrt{\left(1-\psi^2/2\right)^2+2\psi^2-1}\quad-1 \tag{11}$$

Fig. 2 presents the graphical representation of Eq. (10), where the parameter z is plotted along the vertical axis and the parameter ψ along the horizontal axis.

Fig. 2 presents a graphical interpretation of the analytical relationship derived in Eq. (10), illustrating the behavior of the dimensionless downstream depth ratio $z = h/s$ as a function of the dimensionless parameter ψ. This plot plays a central role in identifying and characterizing the flow regime - *submerged* or *unsubmerged* - across a small overflow dam. Specifically, it corresponds to the limit case where the upstream water depth equals the dam height, i.e., $h_1 = s$ (Fig. 1). The curve thus represents the limit of submergence**, i.e.,** the boundary condition separating *submerged* flow from *unsubmerged* (free) flow. The curve demonstrates a monotonically increasing trend, which indicates that as the flow intensity increases (via a higher ψ), the normalized downstream depth z also increases. This behavior is consistent with physical intuition: a higher unit discharge q requires a deeper downstream flow to conserve energy under *submerged* conditions.

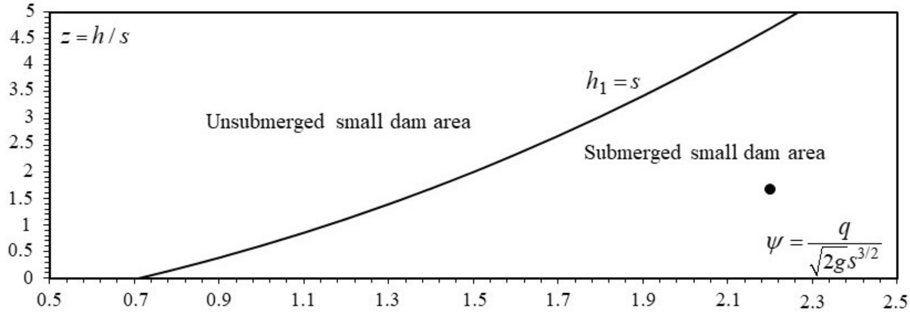

Figure 2: Hydraulic conditions of the *submerged* small dam. Curve generated based on Eq. (10) corresponding to $h_1 = s$. (•) Practical case corresponding to $z = h/s = 1.656$; $\psi = 2.2$

The practical use of Fig. 2 is as follows. Each pair of values (ψ, z) identifies a unique hydraulic configuration. By plotting this pair as a point on the graph: 1) If the point lies to the left of the curve $h_1 = s$, the dam operates under free-flow (*unsubmerged*) conditions. This means the upstream water depth h_1 (Fig. 1) is less than the crest height s, and the downstream water level has no influence on the discharge; 2) Conversely, if the point lies to the right of the curve $h_1 = s$, the dam is under *submerged* flow conditions. This occurs when the downstream depth begins to influence the upstream conditions, thereby reducing the discharge compared to the free-flow regime.

As an illustrative example, a practical case corresponding to $z = h/s = 1.656$ and $\psi = 2.2$ is plotted in Fig. 2. The resulting point lies to the right of the curve defined by $h_1 = s$, thereby confirming that the small dam operates under *submerged* flow conditions.

This graphical approach provides a valuable diagnostic tool. By calculating the values of ψ and z from known hydraulic parameters, practitioners can determine the flow regime without solving the full set of governing equations. It also clearly demarcates the transition zone between *submerged* and *unsubmerged* conditions.

Ultimately, Fig. 2 serves as a powerful design aid. It validates the theoretical framework developed in the study and offers a practical method to assess submergence conditions for small overflow dams using only basic hydraulic parameters. Its elegance lies in condensing the complex interaction of discharge, flow depth, and dam height into a single, easy-to-use chart.

This reinforces the utility of the graph as a decision tool for field engineers and designers. By calculating ψ from known flow parameters, one can quickly determine whether submergence will occur and estimate the downstream depth in dimensionless form, avoiding the need for complex iterative solutions or empirical adjustments. However, Fig. 2 is limited in terms of the range of z and ψ. If a given problem involves a broader range of these parameters, it is advisable to refer to Fig. 3.

Alternatively, another equally simple method can be employed to determine whether the small dam is *submerged* or *unsubmerged*. This involves directly comparing the left- and right-hand sides of inequality (11), provided that z and ψ are known. In this regard, it is straightforward to verify that the point plotted in Fig. 2, with coordinates (2.2; 1.656), satisfies inequality (11), thereby confirming that the small dam operates under *submerged* flow conditions.

DOWNSTREAM DEPTH RATIO

This term typically refers to the ratio of the downstream water depth h_1 to a characteristic length, such as the dam height s (Fig. 1). Let us define herein the downstream depth ratio w as follows:

$$w = \frac{h_1}{s+h} \tag{12}$$

where $0 \le w < 1$. The configuration corresponding to $w = 1$ is not practically feasible, as the free surface cannot remain horizontal downstream of the dam due to energy losses caused by friction along the downstream face of the structure. Note that for the sake of computational simplicity, the effects of frictional losses are neglected in this analysis, acknowledging that such losses are not readily quantifiable. By substituting Eq. (12) into Eq. (3), and introducing the unit discharge q, yields to express the following:

$$s + h + \frac{q^2}{2g\,(s+h)^2} = w\left(s+h\right) + \frac{q^2}{2g\,w^2\left(s+h\right)^2} \tag{13}$$

After simplification and rearrangement, Eq. (13) reduces to the follows:

$$\left(1+z\right)^3 = \psi^2 \,\frac{1+w}{w^2} \tag{14}$$

Eq. (14) is a second-degree equation in w, expressed as follows:

$$w^2 - \frac{\psi^2}{\left(1+z\right)^3}\,w - \frac{\psi^2}{\left(1+z\right)^3} = 0 \tag{15}$$

The discriminant of Eq. (15) can be written as follows:

$$\Delta = \frac{\psi^2\left[\psi^2 + 4\left(1+z\right)^3\right]}{\left(1+z\right)^6}$$

One may thus observe that the discriminant Δ is positive. The real root of Eq. (15) is therefore given by the following:

$$w = \frac{\psi}{2(1+z)^3}\left(\psi + \sqrt{\psi^2 + 4(1+z)^3}\right) \tag{16}$$

Eq. (16) thus comprises the three dimensionless parameters previously defined, namely: w, ψ, and z. For known values of the parameters ψ and z, Eq. (16) allows for the explicit calculation of the downstream depth ratio w of the small dam. This relationship has been plotted in Fig. 3, yielding a series of curves corresponding to fixed values of the downstream depth ratio w.

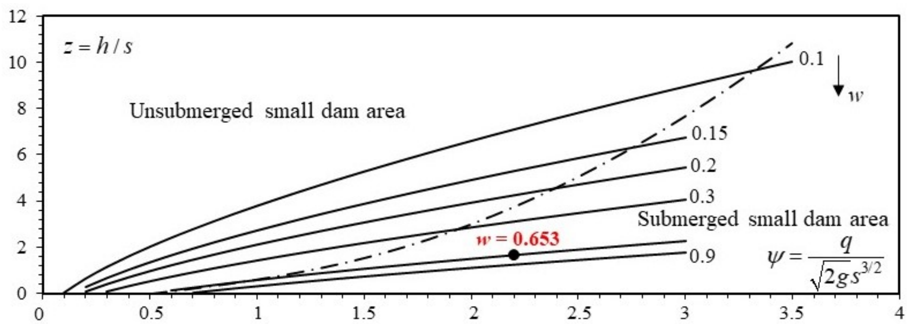

Figure 3: Plot of Eq. (16) for fixed values of the downstream depth ratio *w*. (- - -) Limiting curve of the *submerged* small dam plotted according to Eq. (10). (●) Practical case corresponding to *z* = 1.656; *ψ* = 2.2

The chart of Fig. 3 serves as a valuable hydraulic diagnostic tool by mapping out a set of curves corresponding to different values of the downstream depth ratio w. The plotted curves each correspond to a fixed value of w, illustrating how variations in ψ and z affect the hydraulic behavior of the structure.

The family of curves plotted in Fig. 3 illustrates how variations in ψ and z affect the submergence conditions of the small dam. Each curve represents a unique hydraulic configuration characterized by a constant value of w. As ψ increases, which implies greater unit discharge intensity, the required relative upstream depth z also increases to maintain the same downstream depth ratio w. This behavior is consistent with hydraulic theory: more energetic flows demand increased upstream depths to preserve the downstream flow characteristics under *submerged* conditions.

A key feature of Fig. 3 is the inclusion of the limiting curve, represented as a dashed line, which delineates the threshold beyond which submergence begins to occur. This boundary condition corresponds to the limit derived in Eq. (10) and serves as a reference to determine whether a given configuration leads to *submerged* or free-flow conditions.

Moreover, a specific practical case is plotted on Fig. 3 with coordinates (2.2; 1.656), indicated by a black dot. This point lies to the right of the limiting curve, confirming that under the given flow and geometric conditions, the small dam operates in a *submerged* state. The ability to visually verify submergence without iterative calculations enhances the utility of Fig. 3 for engineers and practitioners.

In other words, Fig. 3 reinforces the robustness and applicability of the theoretical developments presented in the study. It provides a clear, graphical framework for understanding and predicting submergence phenomena in small overflow dams. Its simplicity, rooted in dimensionless analysis, ensures it can be applied efficiently in both academic contexts and field engineering practices.

Furthermore, for small values of $z = h/s$, the curves tighten or converge, which means that the changes in w become minimal even as ψ varies. This implies that, in this range, the downstream influence, embodied in w, is relatively insensitive to variations in flow intensity. Specifically, as depicted in Fig. 3, the curves for $w = 0.653$ and $w = 0.9$ are visibly very close to each other, indicating that the submergence condition is nearly identical despite a significant difference in nominal w values. This reinforces the idea that small upstream depths relative to dam height result in a narrow band of downstream responses.

This behavior is fully consistent with the definition of w in Eq. (12), because when $h \ll s$, the denominator $(s + h) \approx s$, and small changes in h, or in h_1, have limited effect on the value of w. The physical meaning is that in highly submerged conditions with shallow upstream flow, the influence of flow intensity on downstream depth becomes minimal, which is exactly what the convergence of the curves in Fig. 3 illustrates. So, the convergence of curves in Fig. 3 is due to the reduced sensitivity of w to variations in ψ, i.e., in q, not because w is invariant. Indeed, it is worth noting that, for small values of $z=h/s$, or $h \ll s$, Eq. (12) may be approximated by $w \approx h_1/s$. In this regime, even as the unit discharge q - and consequently the flow intensity ψ - increases, the downstream depth ratio w exhibits limited variation. This results in a visible convergence of the curves in Fig. 3, indicating a reduced sensitivity of the flow configuration to changes in discharge. Such behavior highlights a hydraulically stable zone where the impact of increasing flow on downstream conditions becomes minimal. In the regime where $z = h/s \ll 1$, and particularly when the flow is submerged, the geometry of the structure with large s tends to dominate the influence of increasing unit discharge q or the unit discharge intensity ψ. As a result, the increase in h_1 as q increases is limited, meaning h_1 grows more slowly than in non-submerged or transitional conditions. Hence, the variation in h_1 with respect to increasing ψ is relatively small, leading to quasi-horizontal curves or closely spaced curves in Fig. 3 for constant w.

This convergence at low z values reveals a critical regime where the dam's geometric and hydraulic constraints limit the differentiation between flow states, making it a sensitive design zone. Engineers should be particularly cautious in this region, as minor changes in upstream conditions may not yield substantial variation in downstream behavior, possibly complicating efforts to control or predict submergence.

Thus, Fig. 3 vividly demonstrates the robustness of the theoretical model in capturing nuanced flow behavior and provides a practical graphical tool for field application. The observed convergence of curves at small z supports the model's consistency and reveals important hydraulic insights about the influence (or lack thereof) of flow intensity under shallow upstream conditions.

By combining Eqs. (12) and (16), the following relationship is obtained, allowing for the determination of the downstream flow depth h_1 at the toe of the small dam, as illustrated in Fig. 1:

$$h_1 = \frac{s}{2} \frac{\psi}{\left(1+z\right)^2} \left(\psi + \sqrt{\psi^2 + 4\left(1+z\right)^3} \right) \tag{17}$$

where $0 \le h_1 < \left(s+h\right)$

Eq. (17) is applicable to small dams where the effect of frictional losses along the downstream face is negligible. It enables computing the downstream flow depth at the toe of the small depth, using only a minimal set of known key parameters, namely, the unit discharge, the upstream depth, and the dam height, translating into dimensionless variables. By capturing the complex interplay between flow depth and structure geometry in a dimensionless framework, the equation enhances both analytical accuracy and practical decision-making in hydraulic design. Moreover, Eq. (17) aids engineers in plotting backwater curves while estimating their nature and effects (Achour and Amara, 2021; Achour et al., 2022a), designing stilling basins (Achour et al., 2022b; 2022c), the exactness in determining the radius of curvature of the downstream toe of a spillway (Houichi and Achour, 2021), and understanding the energy profile downstream of the dam (Hazzab and Chafi, 2006), where the flow depth at the dam's toe constitutes a critical hydraulic parameter.

For larger structures, where such frictional losses cannot be disregarded, the downstream flow depth h_1 can be determined by referring to the study conducted by Houichi and Achour (2007). The study is based on field data documented in the scholarly literature, thereby accounting for the effects of frictional losses.

SUBMERGENCE RATIO

The submergence ratio can be defined by the parameter β, expressed as follows:

$$\beta = \frac{h_1 - s}{h} \tag{18}$$

The submergence ratio β serves as a critical design and diagnostic parameter. It encapsulates complex flow interactions into a compact and usable form, reinforcing the study's objective of offering practical, theoretically grounded tools for analyzing *submerged* small dam behavior.

The submergence ratio β, as defined in Eq. (18), represents a key dimensionless parameter for characterizing the hydraulic regime over a small overflow dam. This ratio quantifies the degree to which the downstream water level influences the upstream flow and, consequently, the overall discharge behavior of the structure. It offers a precise and intuitive indicator of whether the dam is operating under *submerged* or free-flow conditions. A β value approaching unity or greater typically indicates significant downstream influence, corresponding to a *submerged* flow regime, whereas lower values denote *unsubmerged* conditions where the downstream level exerts little or no control over discharge.

In hydraulic engineering, such a ratio is especially useful for practical diagnostics and design. Given known geometric and hydraulic parameters (e.g., dam height, upstream flow depth, unit discharge), engineers can determine β either through theoretical calculations or graphically. This facilitates informed decisions regarding dam efficiency, energy dissipation requirements (Benmalek and Debabèche, 2022), and backwater effects.

Furthermore, Eq. (18) provides an accessible means for integrating theoretical results into field applications. By combining β with the previously developed analytical framework, including dimensionless parameters ψ, z, and w, one can evaluate the operational status of small hydraulic structures without relying on empirical calibrations.

Inserting Eq. (12) into Eq. (18), and introducing the dimensionless parameters w and z, yields the following relationship:

$$\beta = \frac{w(1+z)-1}{z} \quad (19)$$

On the other hand, inserting Eq. (16) into Eq. (19), one may obtain the following relationship:

$$\beta = \frac{\psi}{2z(1+z)^2}\left(\psi + \sqrt{\psi^2 + 4(1+z)^3}\right) - \frac{1}{z} \quad (20)$$

For the given value of both ψ and z, Eq. (20) may yield negative, zero, or positive values for the submergence ratio β. These values correspond to the following flow configurations:

- $\beta < 0$, corresponding to $h_1 < s$ according to Eq. (18). This configuration corresponds to an *unsubmerged* (free-flow) small dam.

- $\beta = 0$, corresponding to the configuration of an *unsubmerged* small dam, where the downstream flow depth h_1 is equal to the dam height s, i.e., $h_1 = s$, in accordance with Eq. (18).
- $\beta > 0$, corresponding to $h_1 > s$ in accordance with Eq. (18). The small dam is *submerged*.

Given the known values of w and z, Eq. (20) allows for the explicit calculation of the submergence ratio β. This enables the determination of whether the small dam is operating under *submerged* or *unsubmerged* conditions, based on the calculated value of β, as previously outlined.

Thus, from a practical engineering perspective, the submergence ratio β serves as a decisive criterion for classifying the operational status of small overflow dams. Its utility lies not only in diagnosing flow regimes but also in informing design choices and operational strategies. When applied to field situations, the explicit formulation of β (Eq. 20) provides a rapid and reliable means of verifying whether downstream hydraulic conditions are exerting a controlling influence on upstream flow. For instance, during high river discharges or seasonal flood events (Hountondji et al., 2019; Benslimane et al., 2020; Hafnaoui et al., 2022), a sudden increase in the downstream water level may lead to an unanticipated shift from *unsubmerged* to *submerged* flow. By monitoring the variation of β over time, engineers can anticipate such transitions and implement necessary measures, such as adjusting spillway gates or preparing for reduced discharge efficiency. Moreover, β can guide the design of energy dissipation structures and sediment transport management downstream of the dam (Bougamouza et al., 2020; Ansari et al., 2024). A higher β signifies that backwater effects are non-negligible, potentially requiring more robust downstream protection works. Conversely, a low β may indicate conditions favorable for maximizing discharge capacity without compromising structural integrity. In sum, the parameter β transcends theoretical abstraction. It is a practical, actionable tool for engineers engaged in the design, assessment, and operation of small hydraulic structures, especially in contexts where reliable, rapid assessments of flow regime are essential.

CONCLUSION

This study presents a rigorous theoretical investigation into the hydraulic conditions governing flow over *submerged* small overflow dams, offering a significant contribution to the field of hydraulic engineering. By employing fundamental energy principles and adopting a dimensionless approach, the research successfully derives explicit analytical formulations that characterize the transition between *submerged* and free-flow conditions. Central to this development are three key dimensionless parameters, namely, ψ (representing flow intensity), z (upstream depth ratio), and w (downstream depth ratio), which enable a compact and generalized representation of the hydraulic regime.

The study introduces a unique predictive framework grounded in a second-degree equation that delineates the operational boundary of *submerged* small dams. This approach leads to the derivation of a simple, yet powerful criterion to determine whether a small dam operates under *submerged* or *unsubmerged* flow. The graphical interpretation of this criterion, through easily interpretable curves, adds considerable practical value. By plotting (ψ, z) coordinates, engineers can immediately diagnose the flow regime, minimizing computational overhead while ensuring analytical precision.

Furthermore, the research defines and quantifies the submergence ratio β, a crucial dimensionless indicator that encapsulates the extent to which downstream conditions influence upstream flow behavior. Its analytical expression, when coupled with other derived relationships, provides a complete and reliable toolkit for hydraulic diagnostics, suitable for operational assessments of small dams, specifically indicating their current operational status.

In summary, this work transcends traditional empirical methods by offering a generalized theoretical model supported by straightforward graphical tools. It addresses a clear gap in the literature related to the hydraulic behavior of *submerged* small dams and proposes a robust methodology that can be seamlessly integrated into engineering practice. The models and relationships established herein enhance predictive capacity and offer engineers a valuable framework for the design, evaluation, and real-time assessment of small hydraulic structures subject to varying flow conditions.

MAIN RESULTS OF THE STUDY

This study provides a robust, theoretically grounded, and practically applicable framework for evaluating the hydraulic behavior of *submerged* small overflow dams. Its dimensionless modeling approach, graphical tools, and analytical precision make it a valuable contribution to hydraulic engineering, especially in areas with limited access to advanced computational tools or empirical calibration data. The work enhances understanding, supports design optimization, and enables reliable field assessment of flow conditions in small dam structures. The following summarizes the main findings of the study:

Identification of a knowledge gap

The literature review reveals a clear deficiency in studies that specifically address *submerged* flow conditions in small overflow dams. Most existing research focuses on thin-crested weirs, often neglecting the transitional flow behaviors or failing to provide criteria to distinguish between *submerged* and free-flow conditions. This paper fills that gap by developing a theoretical and practical framework that characterizes these conditions.

Development of a dimensionless theoretical framework

The study introduces three key dimensionless parameters, namely, ψ a parameter representing unit discharge intensity, z the upstream flow depth relative to dam height, w the downstream depth ratio. These parameters form the basis for developing a generalized and scalable approach applicable to a broad range of hydraulic conditions, allowing practitioners to avoid empirical calibrations and directly apply theory-based calculations.

Derivation of explicit criteria for submergence

The authors derive a second-order equation (Eq. 9) whose solution yields a simple and explicit criterion (Eq. 10) for determining whether a small overflow dam operates under *submerged* or *unsubmerged* conditions, improving the results of a previous study (Achour and Houichi, 2019). The critical threshold is represented graphically in **Fig. 2**, providing a single curve that separates the two flow regimes based on the values of ψ and z.

Downstream depth ratio estimation

The study further derives another second-order equation (Eq. 15) that governs the downstream depth ratio $\boldsymbol{w}$, and presents its explicit solution (Eq. 16). This is significant because it enables the calculation of the downstream flow depth from upstream and geometric parameters alone, again using a dimensionless formulation. The results are visualized in Fig. 3**,** which shows how ψ and z determine w for various flow configurations.

In this context, it is worth to highlight the role of Eq. (17)**,** which enables the explicit computation of the downstream flow depth h_1 at the toe of small dams, using only a minimal set of known parameters, namely, the unit discharge, the upstream depth, and the dam height. By translating these key hydraulic and geometric physical parameters into dimensionless variables, the model provides a reliable and theoretically grounded estimate of the downstream depth, bypassing the need for empirical or site-specific calibration.

Hydraulic behavior at low relative upstream depths: Insights from Fig. 3

Fig. 3 offers a clear visualization of the downstream depth ratio w as influenced by unit discharge intensity ψ and the upstream depth ratio $z = h/s$. A notable observation is the convergence of the plotted curves for small values of z, indicating that variations in w become minimal across a wide range of ψ. In particular, as depicted in Fig. 3, the curves for $w = 0.653$ and $w = 0.9$ appear nearly identical, underscoring the reduced sensitivity of downstream flow conditions in this regime. This behavior highlights a critical hydraulic zone where the response of the flow becomes increasingly insensitive to upstream variations, a factor of practical importance in the design and operation of small overflow dams. Fig. 3 thus reinforces the robustness of the theoretical model and provides valuable guidance for interpreting submergence conditions under shallow upstream flows.

In the low-z regime, the downstream submerged depth h_1 varies only slightly with increasing flow intensity, reflecting the flow's reduced sensitivity to discharge changes. This hydraulic stability explains the observed convergence of the curves in Fig. 3.

Definition and use of the submergence ratio (β)

A pivotal contribution is the introduction and formulation of the submergence ratio β (Eq. 18), a parameter that quantifies the degree to which downstream water levels influence upstream discharge conditions. This ratio becomes a decisive tool for classifying flow regimes: $\beta < \mathbf{0}$: free flow, $\beta = \mathbf{0}$: critical threshold, $\beta > \mathbf{0}$: *submerged* flow. Its explicit expression (Eq. 20) allows quick computation and field evaluation, enabling real-time diagnostics in operational contexts.

Practical and graphical utility

Figs. 2 and 3 serve as powerful diagnostic tools. With minimal input, unit discharge, dam height, and upstream depth, engineers can use the plotted curves to identify the operational regime of a dam, estimate downstream depth, and assess the influence of submergence. These graphical tools simplify otherwise complex calculations and enhance field applicability.

Engineering and design applications

Beyond the theoretical developments, the study's outcomes support real-world hydraulic design and monitoring. The findings aid in:

- Determining flow regime transitions during variable discharges (e.g., floods) (Remini, 2023; Ezz, 2025; Do et al., 2025),
- Designing energy dissipation structures (Bentalha and Habi, 2017; Amara et al., 2019; Lebdiri et al., 2020; Brakeni et al., 2021),
- Managing sediment transport and backwater effects (Larfi and Remini, 2006; Meddi, 2015),
- Anticipating reductions in discharge efficiency due to submergence (Amara and Achour, 2020).

Declaration of competing interest

The authors declare that they have no known competing financial interests or personal relationships that could have appeared to influence the work reported in this paper.

REFERENCES

ACHOUR B., BOUZIANE T., NEBBAR K. (2003). Triangular Thick-Walled Flowmeter in a Rectangular Channel (Part one), Larhyss Journal, No 2, pp.7-43. (In French)

ACHOUR B., HOUICHI L. (2019). Hydraulic conditions of submerged small overspill dams, Larhyss Journal, No 38, pp. 49-58. (In French)

ACHOUR B., AMARA L. (2021). New theoretical considerations on the gradually varied flow in a wide rectangular channel, Larhyss Journal, No 47, pp. 87-117.

ACHOUR B., AMARA L., MEHTA D. (2022a). New theoretical considerations on the gradually varied flow in a triangular channel, Larhyss Journal, No 50, pp. 7-29.

ACHOUR B., AMARA L., MEHTA D., BALAGANESAN P. (2022b). Compactness of hydraulic jump rectangular stilling basins using a Broad-crested sill, Larhyss Journal, No 51, pp. 31-41.

ACHOUR B., AMARA L., MEHTA D. (2022a). Control of the hydraulic jump by a thin-crested sill in a rectangular channel - new experimental considerations, Larhyss Journal, No 50, pp. 31-48.

AMARA L., LACHI H., BERREKSI A. (2019). Numerical computation of hydraulic jump by finite element model, Larhyss Journal, No 38, pp. 59-70. (In French)

AMARA L., ACHOUR B. (2020). Discussion of “coefficient of shaft spillway under small heads” by Gouryev A.P., Brakeni A., Beglarova E.C, Larhyss Journal, No 43, pp. 7-11.

ANSARI M.A., DANISH M., HUSSAIN A., AZAMATHULLA H.M. (2024). ANFIS based approach to predict sediment removal efficiency of vortex settling basin, Larhyss Journal, No 59, pp. 193-209.

BAZIN H. (1894). New Experiments on Weir Flow," Vol. VII, Annals of Bridges and Roads, Memoirs and Documents, Paris, France. (In French)

BENMALEK A., DEBABECHE M. (2022). Theoretical and experimental analysis of sequence depth ratio and energy loss in an abruptly enlarged trapezoidal channel, Larhyss Journal, No 40, pp. 67-84.

BENSLIMANE M., BERREKSI A., BENMAMAR S., BOUACH A. (2020). Flood risk numerical simulation of Bejaia city urban zone (Algeria), Larhyss Journal, No 42, pp. 167-178.

BENTALHA C., HABI M. (2017). Numerical simulation of water flow along stepped spillways with non-uniform step heights, Larhyss Journal, No 17, pp. 115-129.

BOS M.G. (1976). Discharge measurement structures, hydraulic laboratory, Wageningen, The Netherlands, Rapport 4, May.

BOUGAMOUZA A., REMINI B., SAKHRAOUI F. (2020). Analytical study of sediment evolution in the lake of the Foum El Gherza dam (Biskra, Algeria), Larhyss Journal, No 43, pp. 169-179.

BRAKENI A., GOURYEV A.P., CHUMICHEVA M.M., MAREEVA O.V., VERHOGLYADOVA A.S. (2021). Study of a stilling basin with a swirling flow, Larhyss Journal, No 46, pp. 115-130.

COX G.N. (1928). The submerged weir as a measuring device, Bulletin engineering experiment station series No 67, University of Wisconsin, Madison, Wisconsin, USA.

DO T.V.H., PHAM H.G., KIEU Q.L., TRAN T.N.H. (2025). The typical mechanisms and factors leading to flash floods in small watersheds in the mountainous region of Vietnam, a case study in the CHU VA stream watershed, Larhyss Journal, No 61, pp. 141-168.

EZZ H. (2025). Unexpected flooding in Mersa Matruh, Egypt - Investigating causes, hydrological analysis, and flood risk assessment, Larhyss Journal, No 371-399.

FALVEY H.T. (2003). Hydraulic design of labyrinth weirs, American Society of Civil Engineers Press, American Society of Civil Engineers (ASCE) Press, Reston, Virginia, USA, ISBN 0-7844-0631-6.

FRANCIS J.B. (1884). Experiments on the flow of water over submerged weirs, Transactions of the American Society of Civil Engineers, ASCE, No 13, pp. 303–312.

FTELEY A., STEARNS F.P. (1883). Description of some experiments on flow of water made during the construction of works for conveying water of Sudbury River to Boston, Transactions of the American Society of Civil Engineers, ASCE, No 12, pp. 101–108.

HAFNAOUI M.A., MADI M., BEN SAID M., BENMALEK A. (2022). Floods in El Bayadh city: causes and factors, Larhyss Journal, No 51, pp. 97-113.

HAZZAB A., CHAFI C. (2006). Experimental investigation of flow and energy dissipation in stepped spillways, Larhyss Journal, No 5, pp. 91-104.

HOUICHI L., ACHOUR B. (2007). Flow depth computation at the toe of an over-flow dam in steeply-sloping case, Dam Engineering, Vol.XVII, Issue 4, pp. 245-256.

HOUICHI L., ACHOUR B. (2021). Dimensionless equation of the radius of curvature of the downstream toe of a spillway, Larhyss Journal, No 47, pp. 133-143.

HOUNTONDJI B., CODO F.P., DAHOUNTO S.V.H., GBAGUIDI T.B. (2019). Flood management in urban environment: case of the Cotonou city in Benin, Larhyss Journal, No 39, pp. 333-347. (In French)

LARFI B., REMINI B. (2006). Solid transport in the Oued Isser watershed impact on siltification of the Beni Amrane dam (Algeria), Larhyss Journal, No 5, pp. 63-73. (In French)

LEBDIRI F., SEGHIR A., BERREKSI A. (2020). Steps number effect on hydraulic parameters of flows in stepped spillways, Larhyss Journal, No 42, pp. 41-51.

MEDDI L. (2015). Contribution to the study of sediment transport in northern Algeria, Larhyss Journal, No 24, pp. 315-336. (In French)

REHBOCK T. (1929). Water measurement with sharp-edged overfalls, Journal VdI, Vol. 73, pp. 7-823. (In German)

REMINI B. (2023). Flash floods in Algeria, Larhyss Journal, No 56, pp. 267-307.

SIA (Swiss Society of Engineers and Architects) (1936). Contribution to the study of gauging methods, Bulletin 18, Schweizer Wasserforschung, Bern, Switzerland. (In French)

VILLEMONTE J.R. (1947). Submerged weir discharge studies, Engineering News-Record, Vol. 139, No 26, pp. 54–56.